

Unexpected Effect of Charge Density of the Aromatic Guests on the Stability of Calix[6]arene–Phenol Host–Guest Complexes

Sándor Kunsági-Máté,^{*,†} Kornélia Szabó,[†] István Bitter,[‡] Géza Nagy,^{†,||} and László Kollár^{§,||}

Department of General and Physical Chemistry, University of Pécs, Ifjúság 6, Pécs, H-7624, Hungary,

Department of Organic Chemical Technology, Budapest University of Technology and Economics,

Budapest 1111, Hungary, Department of Inorganic Chemistry, University of Pécs, Ifjúság 6, Pécs, H-7624,

Hungary, and MTA-PTE Research Group for Chemical Sensors, Ifjúság 6, Pécs, H-7624, Hungary

Received: January 6, 2005; In Final Form: April 6, 2005

The π – π interaction-based inclusion complexation of calix[6]arene hexasulfonate as host with neutral aromatic guest molecules was studied in aqueous media. To vary the electron density on the guest's aromatic rings, the phenol parent compound was functionalized in the para-position with different electron-withdrawing groups, such as NO₂ and Cl, as well as H and CH₃ groups. To study the interaction between calixarene and the guests, PL, DSC, and quantum-chemical methods were used. The results indicate 1:1 stoichiometry for all examined host–guest complexes. Although the enthalpy change predicts strong interaction between the host and the guest, the Gibbs free energy change of the complex formation is small, resulting in a relatively low complex stability. This property is due to the high and negative entropy change during the complex formation. Comparing the thermodynamic parameters observed on the series of the guests, we observed a decrease of the enthalpy change when the electron density on the guest's aromatic ring increased. However, the Gibbs free energy and therefore, the stability of the complexes increased when the enthalpy change lowered. These unexpected results are based on the enthalpy–entropy compensation effect and probably due to the quite different entropy change related to the high and low electron density on the aromatic rings of different guest molecules. Using molecular dynamic calculations, a redistribution of the electron density of calixarene rings, followed by the reordering of the solvent molecules, was identified as a background of this unexpected entropy change at molecular level.

1. Introduction

The recognition of neutral organic molecules by synthetic receptors is a topic of current interest in supramolecular and also in analytical chemistry.^{1,2} Calix[*n*]arenes (*n* = 4–8), cyclic oligomers of phenolic units linked through the ortho-positions, represents a fascinating class of macrocycles, because of the simplicity of their well-defined skeleton, which is associated with versatile recognition properties toward metallic or organic ions and neutral molecules.^{3–5} Recent reviews summarize their thermodynamic⁶ and redox properties,⁷ the extent of their metal ion binding character in solutions,^{8,9} and their wide applications in analytical and separation sciences.¹⁰

The selectivity character of calixarene complexes with different species can be modified by changing the cavity size by the different functionalization at the lower and/or upper rims of the molecule. In our recent papers^{11–13} the complexation behavior and the factors controlling the thermodynamic and kinetic stability or selectivity of some calixarene derivatives toward neutral π -electron deficient aromatics were reported. One of the consequences of those results is that only very weak host–guest complexes of the mentioned molecules can be predicted in water because of its high permittivity.¹³ The stability of the complexes in water can be increased by the assistance of “soft”

Fe(II) ions.¹⁴ These “soft” ions are coordinated first to the aromatic ring of the phenolic unit of the host calixarene.¹⁵ Afterward, calixarene will form a sandwich-type complex with two phenol molecules and the complex stabilized by cation– π interaction. The inclusion complexation of calix[6]arene hexasulfonate with *p*-nitrophenol in aqueous media have been studied recently by PL (photoluminescence), DSC (differential scanning calorimetry), and quantum-chemical methods.¹⁶ The results indicate that the complex has 1:1 stoichiometry and the aromatic guest lies parallel within the two opposite aromatic rings of the calixarene molecule.

The interactions of calixarene with neutral species involve competition between complexation and solvation processes. Nonelectrostatic forces resulting from the interaction of the electronic systems of neutral host and those of neutral guest are of primary importance in “host–guest” interaction. Calixarenes form complexes with electron-deficient neutral aromatics predominantly through π – π type interaction. A quite recent work showed that the complex stability based on the cation– π interaction in metal ion–phenol complexes are highly affected by the substituents connected to the aromatic unit.¹⁷ Comparisons made with other cation– π complexes to benzene showed high influence of the hydroxyl substituent on the binding, and the factors that control the strength of cation– π interactions.

In this work the inclusion complexation of calix[6]arene hexasulfonate as host with neutral aromatic guest molecules as a function of the charge density located on the guest aromatic ring was studied in aqueous media. As model guest molecules, four different phenol derivatives (Figure 1), where the aromatic

* Corresponding author. Tel: +36-72-503600 (-4208). Fax: +36-72-501518. E-mail: kunsagi@ttk.pte.hu.

[†] Department of General and Physical Chemistry, University of Pécs.

[‡] Budapest University of Technology and Economics.

[§] Department of Inorganic Chemistry, University of Pécs.

^{||} MTA-PTE Research Group for Chemical Sensors.

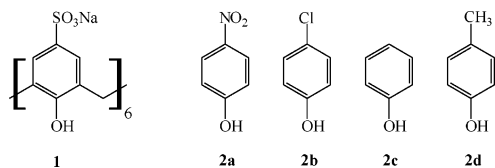


Figure 1. Calix[6]arene–hexasulfonate salt **1** and different phenol derivatives (**2a–d**) chosen as host and guests, respectively: **2a**, *p*-nitrophenol; **2b**, *p*-chlorophenol; **2c**, phenol; **2d**, *p*-methylphenol.

ring was substituted by various substituents in para-position to the OH group, were chosen for this study. The thermodynamic parameters were determined for the complex formation of calix[6]arene **1** with series of phenols **2a–d**. The stoichiometry and the van't Hoff enthalpy of the complex was determined by spectrofluorometric method. The calorimetric molar enthalpy of the inclusion was determined from the heat flow directly measured by DSC method. The fluorometrically determined van't Hoff enthalpy and the calorimetric enthalpy were compared and used for the examination of the two-state behavior of the formation of such a complex. Quantum-chemical investigations were carried out to determine the stable conformation of the host–guest complex. Particularly, the unexpected entropy change was evaluated and interpreted as the influence of the molecular environment of the interacted species.

2. Experimental Section

Calix[6]arene–hexasulfonate salt (**1**) was prepared by the direct sulfonation of the parent calix[6]arene with concentrated sulfuric acid.¹⁸ The guests, *p*-nitrophenol (**2a**), *p*-chlorophenol (**2b**), phenol (**2c**), and *p*-methylphenol (**2d**) (p.a. grade) were purchased (Merck, Germany) and used without further purification.

The acid–base equilibria in the solutions of calixarene **1** were studied by potentiometry using a combined pH sensitive glass electrode (Triode pH electrode, ORION) and Orion 420 Aplus pH meter. The potentiometric measurements were carried out at 298.16 ± 0.1 K. The protonation was studied in an aqueous solution of **1** at concentration of 10^{-2} M with ionic strength of 0.1 M tetraethylammonium perchlorate ($[\text{Et}_4\text{N}][\text{ClO}_4]$) background salt. The estimated error of the pH measurements was found to be about 0.02 pH unit. Values of the stepwise protonation constants K_i and the overall protonation constants β_i were computed with the HyperQuad 2000 (Protonic Software) computer program.^{19–21} Titrations and calibrations were carried out in a glass cell furnished with a thermostating jacket at a temperature of 298.16 ± 0.1 K. A nitrogen stream was used to remove dissolved O_2 and CO_2 . The titrating solutions were added from a standard microburet. The glass electrode was calibrated at a constant ionic strength following the procedure described in the literature.^{22,23} Slopes were within 3% of the theoretical Nernst value, and square regression coefficients for the Nernst type equation were always better than 0.998.

Both fluorometric and calorimetric experiments were carried out at pH ~ 6.9 using phosphate buffer: 0.025 mol/kg disodium hydrogen phosphate (Merck) + 0.025 mol/kg potassium dihydrogen phosphate (Merck); pH 6.961, 6.912, 6.873, 6.843, 6.823, 6.814 at temperatures of 273, 283, 293, 303, 313, 323 K, respectively/

The PL measurements were performed on the Fluorolog $\tau 3$ spectrofluorometric system (Jobin-Yvon/SPEX). For data collection a photon counting method with 0.2 s integration time was used. Excitation and emission bandwidths were set to 1 nm. A 1 mm layer thickness of the fluorescent probes with front face detection was used to eliminate the inner filter effect.

Calorimetric measurements were carried out with a highly sensitive nano-II-DSC 6100 (Setaram, France) instrument. The calorimeter is configured with a platinum capillary cell (volume = 0.299 mL). The samples were pressurized to $(3 \pm 0.02) \times 10^5$ Pa during all scans. Using oil rotation pump, standard degassing procedure for 15 min at about 15 Pa was applied before loading the samples into the capillary. The heat flow was scanned between 273 and 323 K. A typical scanning rate of 0.5 K/min was applied. The effect of diffusion and that on the reaction rate were checked for each sample by varying the scanning rate from 0.1 up to 2 K/min. The experimental deviation of the calorimetric results were estimated to be ± 5 mJ.

To avoid any interaction other than the interaction related to the host–guest complex formation, the DSC curves of solutions of calixarene in buffer (i), calixarene **1** in water (ii), and buffer by oneself (iii) were recorded against water. No significant differences between the curve of summed (ii) with (iii) and that of (i) were obtained, which observation reflects that no considerable interaction between the buffer and the host calixarene exists. A similar result was found for the guest phenol species.

The equilibrium conformations of calixarene **1** and their complexes with phenol derivatives (**2a–d**) were studied with semiempirical AM1 (Austin Model) method, followed by *ab initio* HF/6-31G** calculations. The Fletcher–Reeves geometry optimization method was used for the investigation of the conformers. The interaction energy of the studied species was described at an *ab initio* level using HF/6-31G** calculation. TIP3P method²⁴ with extension to the solvent used²⁵ was applied for considering the solvent effect. The conformation of the complex in water obtained from the above calculations was compared with results derived from the geometry optimization performed at DFT/B3LYP/6-31++G level by using GAUSSIAN 03 package.²⁶ The PCM (Polarizable Continuum Model) method was used to consider the solvent effect. To obtain the equilibrium conformation, the search was started from the positions where either from inside or outside the cavity the guest was located with different orientation to the host molecule.

The temperature-dependent molecular dynamic simulations were performed with AMBER force field. The TIP3P method is used to consider the solvent water molecules explicitly. For this calculation a cubic box with 20 Å side length is used. The box contained 265 water molecules according to the water density at 298 K. To find an appropriate initial condition for molecular dynamics, a “heating” algorithm implemented in HyperChem package was used. This procedure heats the molecular system smoothly from lower temperatures to the temperature T at which molecular dynamics simulation is desired to perform. The starting geometry for this heating phase is a static initial structure. We used the optimized geometry derived from semiempirical AM1 calculations as an initial structure. The temperature step and the time step in the heating phase were set to 2 K and 0.1 fs, respectively. After equilibration at the given temperature, the MD simulations were run in 1 ps time intervals with resolution of 0.1 fs. The simulation time step was 0.1 fs. Ten thousand points were calculated in each run. Five water molecules locating closest to the calixarene's phenolic unit was chosen for data analysis. The inclination angles of the C_2 symmetry axis of the water molecules, related to the directions perpendicular to the planes of the appropriate phenolic units of calixarene molecules, were collected during the simulation. The average values of these angles were used

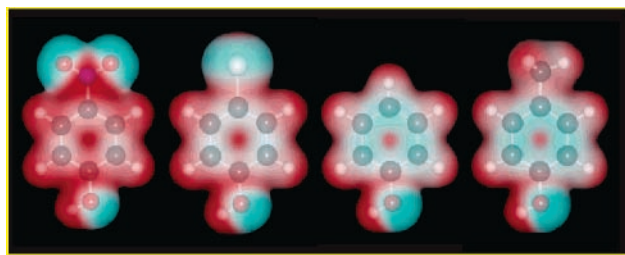


Figure 2. Charge density map of different phenol derivatives (**2a–d**) applied as guests in this study. Calculations were performed with ab initio DFT/6-31G** method.

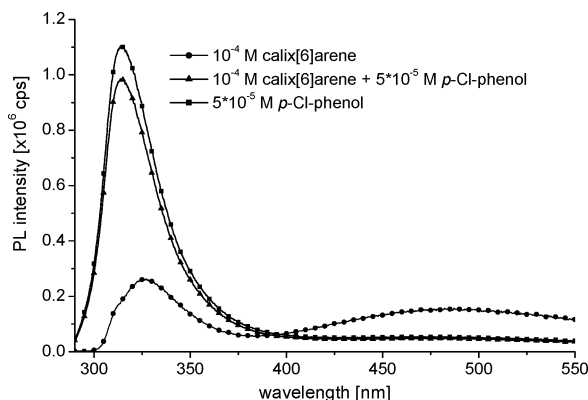


Figure 3. Change of PL spectra of calixarene derivative **1** obtained in the absence (●) and in the presence (▲) of 5×10^{-5} M *p*-chlorophenol and the PL spectra of 5×10^{-5} M *p*-chlorophenol (■).

to represent the freedom of water molecules around the calixarene rings.

Single point calculations and ab initio geometry optimizations were carried out with the GAUSSIAN 03 code,²⁶ and molecular dynamics simulations are performed by the HyperChem Professional 7 program package.²⁷

3. Results and Discussion

To obtain a well-defined protonation state of **1**, the acid–base titration was carried out with adjusting the ionic strength using 0.1 M tetraethylammonium perchlorate background salt.^{5,14} These measurements were carried out under purified nitrogen atmosphere and the experimental details were published elsewhere.^{5,14} The results showed^{5,14} that near pH 7, compound **1** exists in double protonated form. It has to be noted that the distribution curve of CalixH₂⁴⁺ has a wide maximum between pH 6 and pH 8.5, providing excellent conditions for the investigation of its host properties. Because no considerable abundance of other species has been observed at this pH range; therefore, pH \sim 6.9 was chosen for the further examinations. To minimize the effect of the temperature change on pH, phosphate buffer was used which keeps the pH constant at a wide range of temperature (see Experimental Section).

3.1. Effect of Complexation on PL Intensity. To investigate the interaction of **1** with **2a–d**, 10^{-4} M solutions were prepared in phosphate buffer and the PL spectra were recorded. Their evaluation revealed that the guest molecule induced some changes in the spectra. The PL spectrum of **1** exhibits two peaks at 325 and at 485 nm, the intensities of which were decreased in the presence of one from the members of guest series **2a–d** (Figure 3). According to our earlier results,^{5,11–13,15} we supposed that the spectral changes were induced by the formation of an inclusion complex. Because the emission peak of phenols (\sim 310–320 nm) overlaps with the 325 nm peak of **1**, therefore

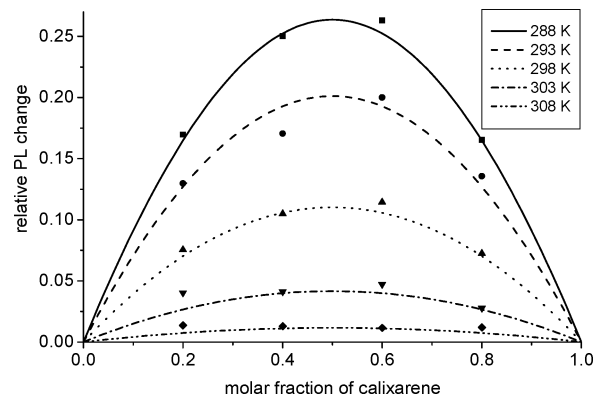


Figure 4. Job's plot of calixarene (**1**) *p*-chlorophenol (**2b**) complexes at different temperatures

TABLE 1: Thermodynamic Parameters of Complexation of 1 with 2a–d

	phenol derivative	ΔG (298 K) (kJ·mol ⁻¹)	ΔH (kJ·mol ⁻¹)	ΔS (J·K ⁻¹ ·mol ⁻¹)
PL	2a	-12.96 (6)	-66.4 (5)	-181.3 (3)
	2b	-21.47 (6)	-61.4 (4)	-134 (5)
	2c	-25.22 (6)	-57.7 (5)	-102 (5)
	2d	-26.27 (6)	-51.3 (4)	-84 (6)
DSC	2a	-13.07 (8)	-68.2 (3)	-185 (9)
	2b	-21.57 (8)	-62.4 (2)	-137 (8)
	2c	-25.32 (8)	-58.7 (3)	-112 (8)
	2d	-26.78 (8)	-53.3 (3)	-89 (8)

the emission of **1** at 495 nm was used to determine the complex stability. Because *p*-nitrophenol (**2a**) also shows considerable emission and its emission band overlaps with the 495 nm band of **1**, in this particular case the 330 nm peak of calixarene was used for the determination of complex stability, as it was described in detail earlier.¹⁴

3.2. Determination of the Stoichiometry and Stability of the Complexes Using Job's Method. Job's method²⁸ is widely used for the spectroscopic determination of complex stability constants also in calixarene chemistry.^{29–33} To determine the stoichiometry of the complexes and thermodynamic parameters of complex formation, 5×10^{-4} M stock solutions of **1** and that of one compound from the phenol derivatives (**2a–d**) were mixed in four different [H]/([G] + [H]) ratios by stepwise addition of $n \times 300 \mu\text{L}$ host to $(5 - n) \times 300 \mu\text{L}$ guest solutions ($n = 1–4$) keeping 5×10^{-4} M total concentration ([G] + [H]). The measurements were carried out at four different temperatures, and the ratios of the change obtained in the PL peak under the effect of guests and those of the bare calixarene solutions were plotted against the molar fraction of calixarene (Figure 4, Job's plot). Figure 4 shows the Job's plot of the calixarene–*p*-chlorophenol detected by the PL method, as representative. In the cases of all different guests, and at all different temperature, Job's curves show a mirror symmetry, indicating the 1:1 complex stoichiometry. Assuming the 1:1 stoichiometry, the thermodynamic properties of the complexation can be calculated. Details of such evaluation of the Job's curves was described earlier.^{12,14,15} Table 1 summarizes the results.

3.3. DSC Measurements on the Host–Guest System. According to our earlier detailed description,¹⁶ the determination of the stability of the host–guest complexes is based on the following treatment. Using the expression of the stability constant K from the van't Hoff equation, the concentration of a 1:1 host–guest complex can be described as a function of the molar enthalpy, entropy change, and of the temperature. The amount of the complex being dissociated, while the temperature

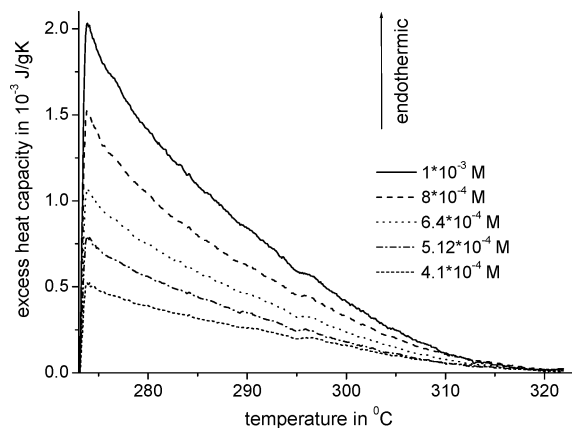


Figure 5. Excess heat capacity of the equimolar solutions of **1** and **2b** scanned with the rate of 0.5 K/min.

increases from 273 to 323 K, can be expressed as the difference of concentrations of the complex at the two temperatures.

To obtain the enthalpy changes during the dissociation of the complex, the excess heat capacities of the equimolar mixture of **1** and **2a–d** were scanned from 273 to 323 K at a rate of 0.5 K/min. Five different concentrations varying between 1×10^{-3} and 4.1×10^{-4} M were applied, keeping the host–guest concentration as the same value at each individual run. As a representative, Figure 5 shows the DSC curves of solutions of **1** with **2b** scanned with the above conditions. The more diluted solutions show lower excess heat capacities at each temperature. Furthermore, the curves display that the excess heat capacity decrease with increasing the temperature for each solution. This is consistent with the theoretical expectations: the amount of complexes, dissociated during the temperature changes in a temperature unit, decreases by increasing the temperature. Accordingly, the measured excess heat capacity decreases with increasing temperature. Overall, this shape of the DSC curves shows that the dissociation process is fast related to the speed of the change of complex concentration, which is induced by the change of temperature at a given scanning rate. Consequently, the system is in quasi-equilibrium state at each temperature. Therefore, the change of the host–guest complex concentration driven by the temperature change is reflected in the DSC curve.

The calculation of calorimetric enthalpies is based on the integration of the area under the excess heat capacity curve. We mention here that the determination of the thermodynamic parameters of the host–guest complexes by DSC method assumes that the heat capacity (c_p) of all individual species involved in the complexation reaction are constant in the temperature range where the measurements are performed.

Figure 6 shows the enthalpy changes of the dissociation plotted against the analytical concentration of equimolar solutions of **1** and **2b**. The solid line shows the change of the complex concentration while the temperature increases from 273 to 323 K. As it is well-known, the concentration of a host–guest complex varies with the temperature as the complex stability constant is affected by the temperature during a DSC run. Therefore, we are unable to determine the concentration of the analyte and consequently, the thermodynamic parameters from a single DSC run.

After the measurements were carried out with five different, however equimolar, concentrations of host and guest, iterative curve-fitting procedure by a variation of ΔH and ΔS was done for the experimental data plotted in Figure 7. Table 1 summarizes the results determined by the procedure described above

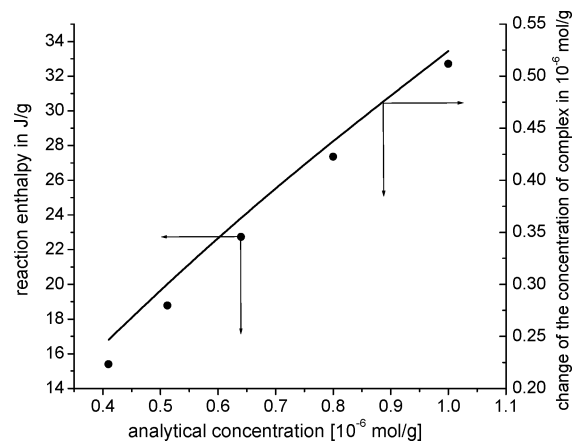


Figure 6. Enthalpy change (●) of decomposition of the host–guest complexes (left axis) plotted against analytical concentration of equimolar solutions of **1** with **2b**. The solid line shows the concentration of the complex dissociated (right axis) while the temperature increased from 273 to 323 K.

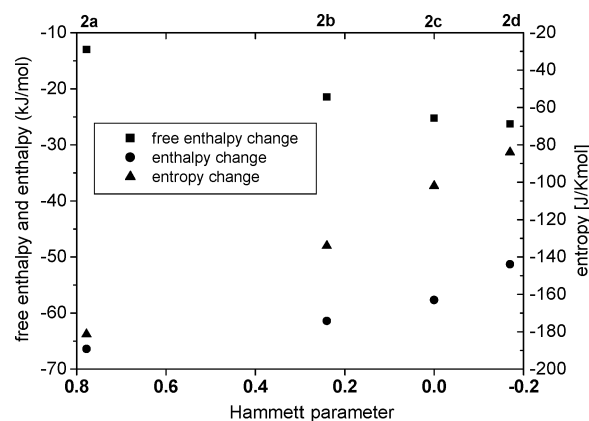


Figure 7. Free enthalpy (■) and enthalpy (●) changes (left axis) and entropy (▲) changes (right axis) measured for the formation of the host–guest complexes as function of the Hammett substituent constants³⁴

using the data of the DSC measurements. It has to be noted that the enthalpy and entropy values in Table 1 are the averaged values over the temperature interval between 273 and 323 K, where the complexation/decomplexation process is studied.

3.4. Comparing the Thermodynamic Parameters of Complex Formation of **1 with Different Guests **2a–d**.** Table 1 and Figure 7 summarize the thermodynamic parameters of the host–guest formation of the calixarene **1** with different phenols. In Figure 7, the Hammett parameter is used as the quantitative property of the electron-withdrawing and electron-releasing feature of the substituents on the aromatic ring of phenols.³⁴ It can be clearly seen that the Gibbs free energy change, and therefore the stability of the host–guest complex, increase with the electron density of the aromatic rings of the guest molecules. Note that all thermodynamic values reflect to the formation of the complex; i.e., the values in the Table 1 show the Gibbs free energy of the complex (product) subtracted with the Gibbs free energy of the separated species (reactants). These values are negative. Because the dependence of the enthalpy change on the mentioned electron density shows opposite tendency, the stability of the complex can be increased only if the entropy would compensate the decrease of the enthalpy changes. However, the entropy change of the complex formation is also negative showing a more ordered structure after the complex was formed. Consequently, the entropy term of the complexation decreases the complex stability. But, the entropy change

decreases fast with the electron density of the aromatic rings of the different guests and this change overcompensates the stability-decreasing effect of enthalpy.

Overall, the highly exothermic complexation enthalpy, parallel with the significant decrease of the entropy change during complex formation, reflects to the so-called enthalpy–entropy-compensation effect. It is probably due to the increased order of guest molecules relative to the host calixarenes and also due to the increased order of solvent molecules after the complex has been formed. However, the negative entropy change during complex formation is an astonishing behavior in this particular case, especially if we consider the following. Before the complex formation both calixarene and the guest molecules are solvated, and the solvent molecules around the solutes are ordered. During the complexation, before the guest phenol molecule enters into the calixarene cavity, it has to lose its solvation shell and also, the solvent molecules have to leave the calixarene cavity. The disorder, and therefore the entropy of the system, considerably increases during this process. Then, the guest molecule enters into the calixarene cavity forming higher ordered conformation. This latest process slightly decreases the entropy. Consequently, in contrast to our present results, the entropy of the system would have to be increased after a host–guest formation.

Because of this surprising result, we examined the complex formation at molecular level using quantum-chemical calculations, too. The interaction energy between the host and the guest molecules was calculated by the procedure described earlier.¹³ All energies were determined in the presence of solvent cage using TIP3P method;^{24,25} i.e., the solvation enthalpies of the interacting species were considered in this way. To obtain the equilibrium conformation, the search was started from the positions where either from inside or outside the cavity the guest was located with different orientation to the host molecule. Only those conformations with the phenol derivatives located inside the calixarene cavity (i.e., phenol interacts with calixarene from the side of the upper rim) were found stable. The orientation of different phenol derivatives inside the calixarene cavity was found to be always the same: para-substituents are located at the top and the phenolic OH at the bottom. The same structure was found when the calculations were repeated at DFT/B3LYP/6-31++G level with the PCM (polarizable continuum model) method to consider the solvent effect. The stabilization energy of the complex was evaluated as the absolute value of the interaction energy. The interaction energy was defined as the difference between the total energy of the optimized structure of the complex and that of the separated host plus guest molecules. Figure 8 shows the top and side view of the optimized structure of the host–guest complex. The phenol molecule enters into the calixarene cavity and lies between the two aromatic rings of the calix[6]arene. The three parallel aromatic rings form a sandwich-type structure. Results confirm that this structure is stabilized either by the π – π interaction or by hydrogen bonds between the aromatic rings or the OH groups of the phenolic units of host and the guest, respectively. The related molecular dynamics calculations showed that the solvent water molecules, which lie in the outer side of the calixarene rings involved into the complex formation, have much higher ordered structure after the guest entered into the cavity (Figure 9). For quantitative description, the angles of the C_2 symmetry axis of the water molecules relating to the directions perpendicular to the planes of the appropriate phenolic units of calixarene molecules were collected during the simulation. The deviation from the average values of these angles of five water molecules closest to the appropriate phenolic ring of calixarene

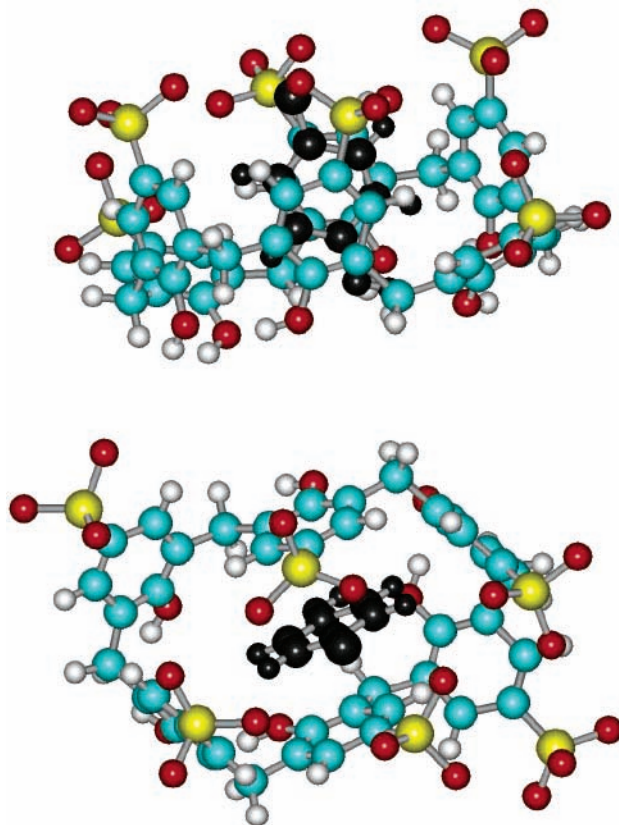


Figure 8. Two views on the optimized structure of the inclusion complex of **1** with **2b**. The phenol molecule (black) enters into the calixarene cavity and lies between the two aromatic rings of the calix[6]arene. The orientation of different phenol derivatives inside the calixarene cavity was found to be always the same: para-substituents are located at the top and the phenolic OH at the bottom. The three parallel aromatic rings form a sandwich-type structure.

were used to represent the freedom of water molecules around the calixarene rings. It was found that the average rotation of the water molecules is nearly three times less in the case when the *p*-nitrophenol guest with its charged aromatic ring is entered into the cavity (85°). (The average rotation value for the nearly neutral *p*-methylphenol is 265°.)

To obtain a microscopic view about the solvent water molecule, their orientation was examined by molecular dynamic calculations at that temperature, where the host–guest complex is desired to form. Figure 9 shows a schematic summary of the results. Accordingly, a recent work showed that the water molecules are coordinated mainly to the OH group of the phenols.³⁵ However, increasing the coordination number, the coordination becomes more and more close to the other atoms in the aromatic ring.³⁵ Because of this coordination stabilized by the $\text{OH}\cdots\pi$ bonds, it is obvious that the change in the aromaticity of the phenol molecule will induce changes in the ordering of the water molecules in the molecular environment. However, the electron density of the calixarene rings is modified when a charged guest molecule enters into the cavity. As a result, a more ordered structure was formed when the aromatic ring of the guest molecule was more charged (Figure 2). Consequently, the more charged the aromatic ring of the guest molecule, the higher the entropy change of the complex formation.

4. Conclusion and Summary

Complexation ability of calix[6]arene hexasulfonate host molecule toward different guest phenol derivatives was studied

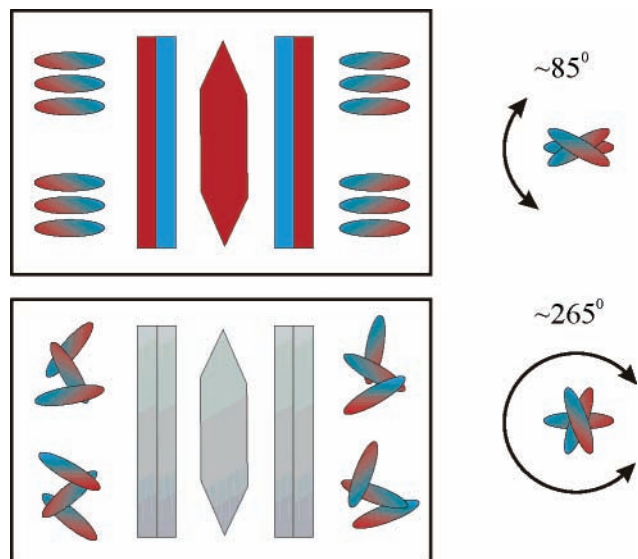


Figure 9. Schematic microscopic view of the entropy change during the complexation of phenols by calixarene. The upper figure is about the complexation of *p*-nitrophenol, where the aromatic ring of the guest molecule is positively charged due to the electron-withdrawing effect of the nitro group. The bottom figure relates to the complexation of phenol, where the aromatic ring is nearly uncharged. The change in the electron density of the calixarene rings results in a higher ordered structure in the former case. The average rotation of the water molecules is reduced when the guest having charged aromatic ring enters into the cavity.

in aqueous solution by PL and DSC measurements and quantum-chemical calculations. According to earlier results, quantum-chemical investigations suggest that the guest molecule resides in the calixarene cavity and the complex is stabilized by π - π interaction between the aromatic rings of the host and that of the guest. To obtain the effect of the electron density of the aromatic ring of the phenol molecules, it was varied by replacing a hydrogen atom in the para-position to the OH group with different electron-withdrawing groups, such as NO_2 and Cl, as well as H and CH_3 groups. Both the PL and DSC signals indicate a 1:1 complex stoichiometry. In all cases the directly measured molar enthalpy of inclusion shows a strong interaction between the host and the guest. However, the entropy change during the complexation is a relatively high negative value, which decreases the Gibbs free energy change of the reaction, thereby the complex stability. The highly exothermic complexation enthalpy parallel with the significant decrease of the entropy during complex formation reflects to the so-called enthalpy-entropy-compensation effect. Furthermore, the electron density of the calixarene rings is modified when a charged guest molecule enters into the cavity. As a result, a more ordered structure is formed when the aromatic ring of the guest molecule is more charged. Overall, the thermodynamic properties of the complex formation show linear Hammett-type correlation. These results are applicable in the development of selective and sensitive chemical sensors for neutral organic aromatics.

Acknowledgment. The financial support of the Hungarian Scientific Research Fund (OTKA Grant TS044800) and that of the joint project of the European Union – Hungarian National Development Program (Grant GVOP-3.2.1-2004-04-0200/3.0) is highly appreciated. Calculations were performed on SunFire 15000 supercomputer located in the Supercomputer Center of the Hungarian National Infrastructure Development Program Office.

References and Notes

- (1) Kuwabara, T.; Nakajima, H.; Nanasawa, M.; Ueno, A. *Anal. Chem.* **1999**, *71*, 2844–2849.
- (2) Beer, P. D.; Gale, P. A.; Chen, G. Z. *Coord. Chem. Rev.* **1999**, *186*, 3–36.
- (3) Gutsche, C. D. *Monographs in Supramolecular Chemistry*; Vol. 1. Calixarenes; The Royal Society of Chemistry: Cambridge, U.K., 1989.
- (4) Gutsche, C. D. *Monographs in Supramolecular Chemistry*; Vol. 6. Calixarenes Revisited; The Royal Society of Chemistry: Cambridge, U.K., 1998.
- (5) Kunsági-Máté, S.; Szabó, K.; Bitter, I.; Nagy, G.; Kollár, L. *Tetrahedron Lett.* **2004**, *45*, 1387–1390.
- (6) Danil de Namor, A. F.; Cleverly, R. M.; Zapata-Ormachea, M. L. *Chem. Rev.* **1998**, *98*, 2495–2525.
- (7) Beer, P. D.; Gale, P. A.; Chen, G. Z. *J. Chem. Soc., Dalton Trans.* **1999**, *12*, 1897–1909.
- (8) Ikeda, A.; Shinkai, S. *Chem. Rev.* **1997**, *97*, 1713–1734.
- (9) Yordanov, A. T.; Roundhill, D. M. *Coord. Chem. Rev.* **1998**, *170*, 93–124.
- (10) Ludwig, R. *Fresenius J. Anal. Chem.* **2000**, *367*, 103–128.
- (11) Kunsági-Máté, S.; Nagy, G.; Kollár, L. *Sens. Actuators B: Chem.* **2001**, *76*, 545–550.
- (12) Kunsági-Máté, S.; Nagy, G.; Jurecka, P.; Kollár, L. *Tetrahedron* **2002**, *58*, 5119–5124.
- (13) Kunsági-Máté, S.; Bitter, I.; Grün, A.; Nagy, G.; Kollár, L. *Anal. Chim. Acta* **2002**, *461*, 273–279.
- (14) Kunsági-Máté, S.; Szabó, K.; Lemli, B.; Bitter, I.; Nagy, G.; Kollár, L. *J. Phys. Chem. B* **2004**, *108*, 15519–15522.
- (15) Kunsági-Máté, S.; Nagy, L.; Nagy, G.; Bitter, I.; Kollár, L. *J. Phys. Chem. B* **2003**, *107*, 4727–4731.
- (16) Kunsági-Máté, S.; Szabó, K.; Lemli, B.; Bitter, I.; Nagy, G.; Kollár, L. *Thermochim. Acta* **2005**, *425*, 121–126.
- (17) Amunugama, R.; Rodgers, M. T. *J. Phys. Chem. A* **2002**, *106*, 9718–9728.
- (18) Shinkai, S.; Mori, T.; Tsubaki, T.; Sone, T.; Manabe, O. *Tetrahedron Lett.* **1984**, *25*, 5315–5318.
- (19) HyperQuad 2000. Ver. 2.1. Protonic Software, 2002.
- (20) Gans, P.; Sabatini, A.; Vacca, A. *Talanta* **1996**, *43*, 1739–1753.
- (21) Alderighi, L.; Gans, P.; Ienco, A.; Peters, D.; Sabatini, A.; Vacca, A. *Coord. Chem. Rev.* **1999**, *184*, 311–318.
- (22) Fiol, S.; Arce, F.; Armesto, X. L.; Penedo, F.; Sastre de Vicente, M. E. *Fresenius J. Anal. Chem.* **1992**, *343*, 469–472.
- (23) Brandariz, I.; Vilarino, T.; Alonso, P.; Herrero, R.; Fiol, S.; Sastre de Vicente, M. E. *Talanta* **1998**, *46*, 1469–1477.
- (24) Jorgensen, W. L.; Chandrasekhas, J.; Madura, J. D.; Impey, R. W.; Klein, M. L. *J. Chem. Phys.* **1983**, *79*, 926–935.
- (25) Bender, T. “Solvent Cage”, Excel Macros to HyperChem, Hypercube, www.hyper.com, 2000.
- (26) Frisch, M. J.; Trucks, G. W.; Schlegel, H. B.; Scuseria, G. E.; Robb, M. A.; Cheeseman, J. R.; Montgomery, J. A., Jr.; Vreven, T.; Kudin, K. N.; Burant, J. C.; Millam, J. M.; Iyengar, S. S.; Tomasi, J.; Barone, V.; Mennucci, B.; Cossi, M.; Scalmani, G.; Rega, N.; Petersson, G. A.; Nakatsuji, H.; Hada, M.; Ehara, M.; Toyota, K.; Fukuda, R.; Hasegawa, J.; Ishida, M.; Nakajima, T.; Honda, Y.; Kitao, O.; Nakai, H.; Klene, M.; Li, X.; Knox, J. E.; Hratchian, H. P.; Cross, J. B.; Bakken, V.; Adamo, C.; Jaramillo, J.; Gomperts, R.; Stratmann, R. E.; Yazyev, O.; Austin, A. J.; Cammi, R.; Pomelli, C.; Ochterski, J. W.; Ayala, P. Y.; Morokuma, K.; Voth, G. A.; Salvador, P.; Dannenberg, J. J.; Zakrzewski, V. G.; Dapprich, S.; Daniels, A. D.; Strain, M. C.; Farkas, O.; Malick, D. K.; Rabuck, A. D.; Raghavachari, K.; Foresman, J. B.; Ortiz, J. V.; Cui, Q.; Baboul, A. G.; Clifford, S.; Cioslowski, J.; Stefanov, B. B.; Liu, G.; Liashenko, A.; Piskorz, P.; Komaromi, I.; Martin, R. L.; Fox, D. J.; Keith, T.; Al-Laham, M. A.; Peng, C. Y.; Nanayakkara, A.; Challacombe, M.; Gill, P. M. W.; Johnson, B.; Chen, W.; Wong, M. W.; Gonzalez, C.; Pople, J. A. *Gaussian 03*, Revision C.02; Gaussian, Inc.: Wallingford CT, 2004.
- (27) HyperChem Professional 7, HyperCube, 2002.
- (28) Rossotti, F. J. C.; Rossotti, H. *The determination of stability constants*; McGraw-Hill: New York, 1961; pp 47–51.
- (29) Inoue, Y.; Yamamoto, K.; Wada, T.; Everitt, S.; Gao, X.-M.; Hou, Z. J.; Tong, L. H.; Jiang, S. K.; Wu, H. M. *J. Chem. Soc., Perkin Trans. 2*, **1998**, *8*, 1807–1816.
- (30) Liu, Y.; Jin, L.; Sun, S.-X. *Microchem. J.* **2000**, *64*, 59–65.
- (31) Liu, Y.; Kang, S.-Z.; Zhang, H.-Y. *Microchem. J.* **2001**, *70*, 115–121.
- (32) Mohammed-Ziegler, I.; Kubinyi, M.; Grofcsik, A.; Grün, A.; Bitter, I. *J. Mol. Struct.* **1999**, *481*, 289–292.
- (33) Okada, Y.; Mizutani, M.; Ishii, F.; Kasai, Y.; Nishimura, J. *Tetrahedron* **2001**, *57*, 1219–1227.
- (34) Jaffé, H. H. *Chem. Rev.* **1953**, *53*, 191–261.
- (35) Kryachko, E. S.; Nakatsuji, H. *J. Phys. Chem. A* **2002**, *106*, 731–742.